PHYSICAL REVIEW B VOLUME 32, NUMBER 10 15 NOVEMBER 1985

Electrical transport in pristine and heavily doped polyacenic materials

Kazuyoshi Tanaka, Shozo Yamanaka, Tsuneaki Koike, and Tokio Yamabe
Department of Hydrocarbon Chemistry, Faculty of Engineering and Division of Molecular Engineering, Graduate School of Engineering, Kyoto University, Sakyo-ku, Kyoto 606, Japan

Katsumi Yoshino and Gaku Ishii
Department of Electrical Engineering, Faculty of Engineering, Osaka University, Yamada-Kami, Suita, Osaka 565, Japan

Shizukuni Yata
Development Laboratories, Kanebo Ltd., Miyakojima-ku, Osaka 534, Japan
(Received 1 March 1985)

Experimental studies of electrical transport properties have been performed with respect to pristine and heavily doped polyacenic materials prepared by pyrolytic treatment of phenol-formaldehyde resin. Four kinds of the pristine samples prepared under different temperatures were employed. It is shown that temperature dependences of electrical conductivity and of thermoelectric power suggest that the conduction mechanism in the samples varies from the three-dimensional variable-range-hopping to the nearly-filled-band metallic regime with increasingly higher values of the chosen pyrolytic temperature.

I. INTRODUCTION

Interest in organic conductive polymers has been growing incessantly in the field of solid-state science ever since the discovery of high electrical conductivity in doped polyacetylene.[1] Extensive studies on pristine and doped polyacetylene have been performed from both experimental and theoretical points of view.[2] However, chemical instability of this substance in air[3] limits the range of its application to electric and/or electronic devices. This limitation promotes interest in air-stable conductive polymers capable of being alternatives to polyacetylene, such as poly(*p*-phenylene)[4] or polythienylene.[5]

In this respect, we have been developing a polyacenic material prepared by pyrolytic treatment of phenol-formaldehyde (PF) resin. This material is stable in air and shows a wide range of electrical conductivity (10^{-11}—10^{0} S cm^{-1} or more), depending on the degree of the carbonization or "graphitization" that is controlled by the pyrolytic temperature applied.[6] Furthermore, it has also been demonstrated for the first time that the doping of this material with either electronic acceptor or donor is effective for the control of conduction carriers and thus causes an increase of the conductivity by 11 orders of magnitude at maximum.[6]

In general, pyrolized polymers have been considered, rather ambiguously, to consist of fractions of various sized condensed aromatic rings like coke or coal and, hence, to be amorphous. It has also been pointed out that the currently studied polyacenic materials show an electron spin resonance peak originating from π electrons as a sort of magnetic impurity.[7] Therefore, a systematic investigation of electrical transport in polyacenic material in the pristine and the doped stages is of interest not only for its own sake, but from the viewpoint of organic amorphous semiconductors. However, there has only been a preliminary report on the temperature dependence of electrical conductivity at high temperatures for undoped pyrolized PF resin.[8]

In this paper we report the results of an experimental study on electrical transport, that is, the temperature dependence of electrical conductivity $\sigma(T)$ and thermoelectric power $S(T)$ of pristine and heavily doped polyacenic materials. Four kinds of typical pristine samples prepared by pyrolytic treatment of PF resin with different temperatures were selected. For dopants, iodine and sodium were employed as electron acceptor and donor, respectively. The doping of all these samples was performed up to each saturation limit. Furthermore, magnetoresistance at low temperature (4.2 K) was examined in pristine and iodine-doped samples with comparatively high electrical conductivity in order to obtain information on their Fermi-energy surfaces.

II. EXPERIMENTAL PROCEDURE

A. Sample preparation

The pristine samples were essentially prepared by pyrolysis of PF resin molded in advance. In the present experiment, fibrous samples were prepared in order to achieve a uniform diffusion of dopants into the texture of the samples. In the molding process, a cloth of PF resin fibers (Kaynol®, from Nippon Kaynol, Inc.) impregnated with a methanol solution of PF resin was pressed under 150 kg/cm^2 at 150 °C after drying of methanol. This molded raw material was pyrolized in a nonoxidative atmosphere.[6,9]

Four kinds of the pristine samples, labeled *B*, *D*, *E*, and *G*, were prepared under very accurate temperature control

 ©1985 The American Physical Society

TABLE I. Pyrolized temperature (T_p in °C) of pristine samples and molar ratios in pristine and doped samples.

Sample	T_p	Pristine [H]/[C] molar ratio	I_2-doped [I]/[C] molar ratio	Na-doped [Na]/[C] molar ratio
B	595	0.35	0.025	0.080
D	650	0.27	0.005	0.058
E	775	0.15	0.022	0.058
G	935	0.05	0.025	0.066

in the range 595—935 °C. In the second and the third columns of Table I are listed the pyrolysis temperatures (T_p) and the [H]/[C] molar ratios determined by elemental analysis with respect to each sample. The values of the [H]/[C] molar ratio indicate the degree of carbonization. The chemistry involved in this pyrolytic treatment has been described in earlier publications.[6] Each sample was made into the form of a plate (ca. 1.5×1.5 cm^2 or less) with thickness of 400—500 μm. These appear as dull black-colored solids due to their fibrous structures, and are insoluble and infusible.

The iodine and the sodium doping was carried out by the conventional techniques described in Ref. 6 until the electrical conductivity was saturated. The [I]/[C] and the [Na]/[C] molar ratios of the doped samples are listed in Table I. The former values were determined by elemental analyses, whereas the latter were determined by titration of the sodium ion after thorough undoping of sodium from the doped sample into water.

B. Electrical conductivity measurements

All the measurements of $\sigma(T)$ were performed by the dc four-probe method except for *B*, to which the dc two-probe method was applied. Measured samples had been cut out into a small rectangular chip (ca. 1×10 mm^2). Silver paste was used to make the electrical contacts onto the pristine samples. For the iodine-doped and the sodium-doped samples Electrodag paint and pressure contact by gold wire were utilized, respectively. The contacted samples were held in a glass container filled with helium after evacuation. The temperature control of the samples was achieved by immersing the container into liquid helium or nitrogen in a Dewar. A mixed solution of ^{4}He and ^{3}He was used for the measurement of low temperatures down to 0.2 K. The measurement of temperature utilized a copper-gold differential thermocouple.

C. Thermoelectric power measurements

Measurements of $S(T)$ were carried out with respect to all the pristine samples and typical iodine-doped samples *D* and *E* (hereafter we abbreviate these as I_2-*D*, I_2-*E*, and so on) over the range 80—290 K.

A square sample (ca. 3×3 mm^2) was mounted between two copper blocks by pressure contacts *in vacuo*. The temperature difference of both ends of the sample chip (ΔT) was set to be ±0.5 °C by alternately heating one of the copper blocks. That is, the thermopower at T was measured by taking an average of those at $(T-0.5, T)$ and $(T, T+0.5)$, where temperatures in parentheses denote those at both ends of the sample. The measurement of temperature utilized an Alumel-Chromel differential thermocouple inserted into holes near the sample in the copper blocks.

D. Magnetoresistance

Measurements of transverse magnetoresistance at 4.2 K were performed with respect to *G* and I_2-*G* cut out into ca. 1×10 mm^2 and immersed in liquid helium. The resistance was measured by the four-probe method described in Sec. II B. The magnetic field applied was in the range 0—63 000 G.

III. RESULTS AND DISCUSSION

A. Conductivity

Temperature dependences of electrical conductivities [$\sigma(T)$] of pristine, iodine-doped, and sodium-doped samples are shown in Fig. 1. Values of σ at room temperature for all the samples are listed in Table II along with the activation energies for conduction (ΔE) estimated at the ini-

TABLE II. Electrical conductivity (σ in S cm^{-1}) at 290 K and activation energy for conduction (ΔE in eV) of pristine and doped samples evaluated from T^{-1} dependence of σ.

Sample	σ Pristine	σ I_2-doped	σ Na-doped	ΔE Pristine	ΔE I_2-doped	ΔE Na-doped
B	1.0×10^{-10}	7.8×10^{-5}	6.1×10^{-3}	3.9×10^{-1}	1.8×10^{-1}	9.7×10^{-2}
D	8.5×10^{-6}	1.0×10^{-3}	3.5×10^{-1}	1.8×10^{-1}	1.2×10^{-1}	6.9×10^{-2}
E	1.2×10^{-1}	3.0×10^{0}	2.9×10^{1}	7.0×10^{-2}	2.9×10^{-2}	1.8×10^{-2}
G	2.7×10^{1}	5.7×10^{1}	4.5×10^{1}	3.6×10^{-3}	3.0×10^{-3}	3.8×10^{-3}

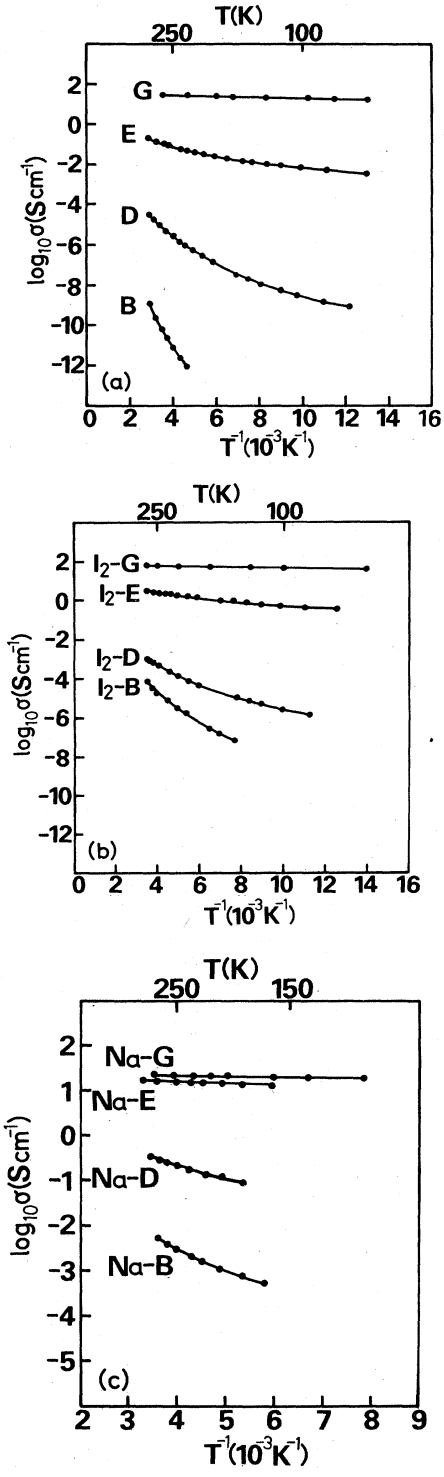

FIG. 1. Conductivity σ vs $1/T$ for (a) pristine samples, (b) I_2-doped samples, and (c) Na-doped samples.

tial slope of the $\log_{10}\sigma$-versus-$1/T$ plots.

It is seen from Fig. 1(a) that progress of the carbonization in the pristine samples gives rise to the increase in σ and the decrease in ΔE, being consistent with the tendency reported earlier.[6,8] The curvature in the plots of B, D, and E in Fig. 1(a) suggests the structural disorder causing a distribution of activation energies. The most carbonized sample, G, shows the activation energy to be smaller than $k_B T$ at room temperature (k_B is Boltzmann's constant) by 1 order of magnitude. Hence G is expected to be rather metallic *per se* in the sense of a nearly filled band structure.

Doping of the pristine samples with iodine or sodium obviously leads to the increase in σ and the decrease in ΔE in almost all the samples. The sodium doping is more effective than the iodine doping in the elevation of σ. The effect of the doping of G is rather small, although the [I]/[C] or [Na]/[C] molar ratios in I_2-G or Na-G are not small. It is noted that σ of Na-E is rather close to that of Na-G but that the magnitudes of ΔE of these two are obviously different, suggesting a structural difference between Na-E and Na-G.

As mentioned above, the curvature seen in the plots in Fig. 1 suggests the existence of disorder in the sample structures. In this respect, the plots of $\log_{10}\sigma$ versus $T^{-1/4}$ are shown in Fig. 2 so as to examine the possibility of the three-dimensional variable-range-hopping (3D-VRH) mechanism[10] governed by

$$\sigma=\sigma_0 \exp\left[-\left[\frac{T_0}{T}\right]^{1/4}\right], \tag{1}$$

where σ_0 is a constant. The selection of the three dimensionality is plausible since there are not well-established layers such as graphite in the structures of the present samples according to preliminary x-ray diffraction analyses.[11]

It is seen from Fig. 2 that the behaviors of $\sigma(T)$ of B, I_2-B, and Na-B (B series) are well fitted by a $T^{-1/4}$ function signifying the effect of the 3D-VRH mechanism in these materials. Other samples (D and E series) do not really show good $T^{-1/4}$ fittings except for the low-temperature data. The G series already demonstrates good linearity with respect to T^{-1} in Fig. 1, and hence the 3D-VRH mechanism is not likely to occur therein as discussed below. On the other hand, the $T^{-1/4}$ dependence of conductivity in the range of rather high temperatures (−50 to 600 °C) has been reported with respect to pyrolized PF resin under various T_p's.[8] The actual behavior of the VRH mechanism, however, should be checked in the lower-temperature region as has been remarked by Mott.[12]

The exponential factor T_0 in Eq. (1) is decomposed into

$$T_0=\frac{16\alpha^3}{k_B N(E_F)}, \tag{2}$$

where α^{-1} is the radius of the localized state wave function and $N(E_F)$ the density of states (DOS) at the Fermi level.[10] In Table III are listed the values of T_0 and $N(E_F)$ estimated from the initial slope of the plots in Fig. 2. For evaluation of $N(E_F)$ we employ a typical value, $\alpha^{-1}=10$ Å, being the order of that estimated for isotropic amorphous carbon film.[13]

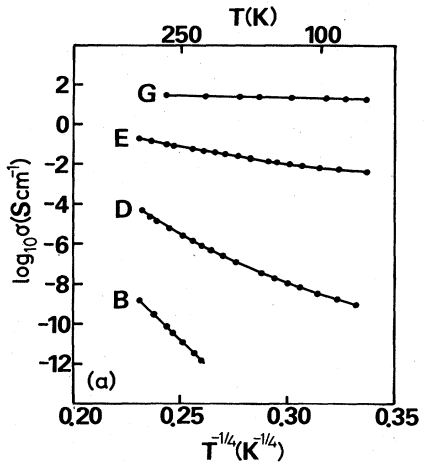

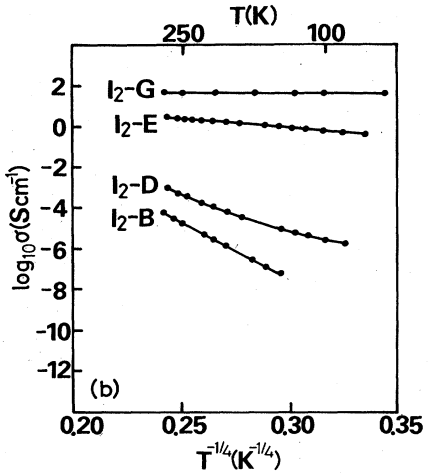

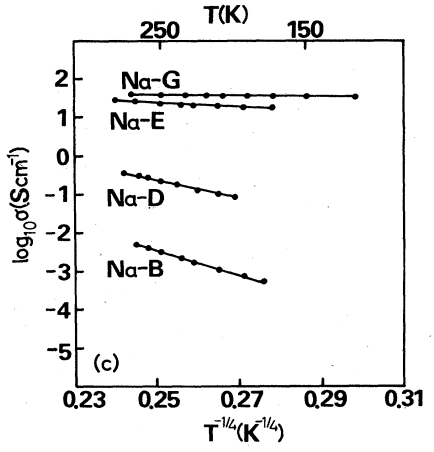

FIG. 2. Conductivity σ vs $(1/T)^{1/4}$ for (a) pristine samples, (b) I_2-doped samples, and (c) Na-doped samples.

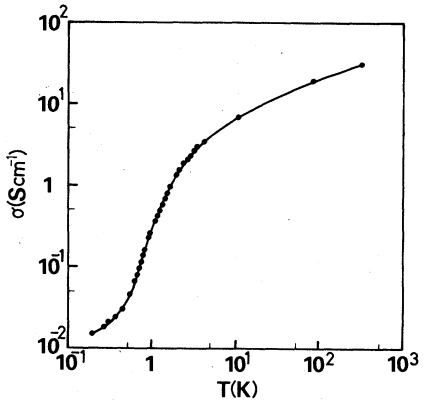

FIG. 3. Low-temperature conductivity of *G*.

Values of $N(E_F)$ thus estimated are in the range 10^{17}–10^{21} states/eV cm^3 (Table III), contrasted with 10^{18} states/eV cm^3 of amorphous carbon film made by sputtering[13] and with 10^{20} states/eV cm^3 of pyrolized poly(*p*-phenylene-1,3,4-oxadiazole) with $T_p = 800$ –1200 °C.[14] Values of $N(E_F)$ of the *G* series in Table III are in excess of 10^{23} states/eV cm^3, which is unrealistic, leading to the conclusion that the 3D-VRH mechanism is not at work in these materials.

The change in σ of *G* down to approximately 0.2 K is shown in Fig. 3. The decrease in σ indicates the conduction mechanism of the activated type is still working at low temperatures in *G*. From this result it can be considered that *G* has a sort of polycrystalline structure mixed with metallic fragments and a less metallic region. Those fragments with high conductivity ought to consist of a well-developed graphitized part, and a small activation energy is required for carrier hopping among these fragments.

B. Thermoelectric power

The results of thermoelectric power *S* versus σ with respect to selected samples measured at room temperature are plotted in Fig. 4. The sign of *S* is positive for all of the measured samples indicative of *p*-type behavior. An increase in σ causes a decrease in *S* monotonically, irrespective of the pristine or the doped states. It is obvious that a semiconductor-metal transition takes place at I_2-*E* or *G* with ΔE less than 3×10^{-2} eV, which is the order of k_BT at room temperature (see Table II). The temperature dependence of *S* is shown in Figs. 5 and 6 except for *B*. The magnitude of *S* in *B* is large (ca. 370 μV/K) and essentially independent of temperature apart from $T^{1/2}$ dependence[10] expected from the 3D-VRH behavior of $\sigma(T)$ in the above. It is noted that pristine *trans*-polyacetylene ($\sigma = 4.4\times10^{-5}$ S cm^{-1})[1] shows a larger value of *S* at room temperature (ca. 900 μV/K), being temperature independent.[15]

The plot of $S(T)$ for *D* in Fig. 5 is instead fitted by a combination of $T^{1/2}$ and *T* functions as

$$S(T) = A\sqrt{T} + BT\ , \tag{3}$$

with $A = 3.83$ and $B = 0.201$. For I_2-*D*, *E*, I_2-*E*, and *G*,

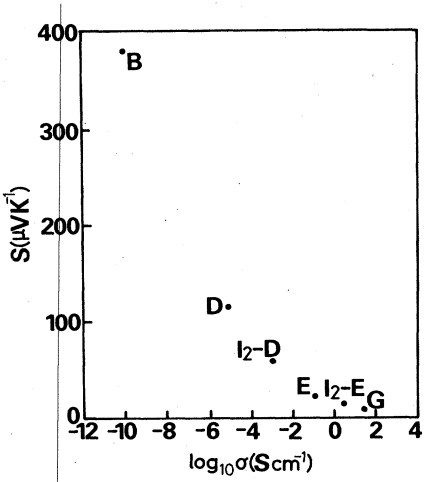

FIG. 4. Thermoelectric power S vs σ for each sample at 280 K.

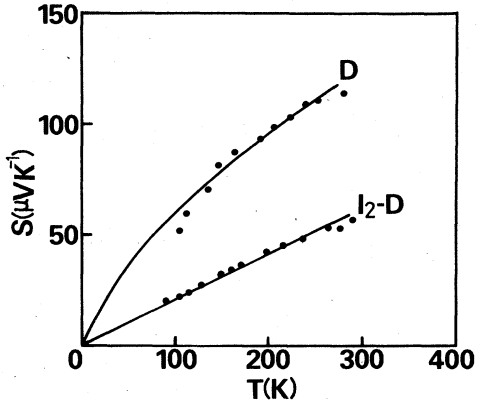

FIG. 5. Temperature dependence of thermoelectric power of D and I_2-D samples. For I_2-D, a fitting curve is $S(T)=0.209T$.

$S(T)$ changes linearly with T, as seen in Figs. 5 and 6, which is characteristic of a nearly-filled-band metallic system. Note that the coefficients of the linear terms in D and I_2-D are almost equal. It should be stressed here that the behavior of $S(T)$ represents the intrinsic nature of the material. Therefore, the actual dc conductivity is limited by the hopping among such metallic fragments as was mentioned in Sec. III A. The nearly-filled-band metallic conduction feature is expected only in these fragments.

The temperature dependence of S in the case of p-type materials is usually analyzed based on the formula[16]

$$S(T)=\frac{\pi^2}{3}\frac{k_B}{|e|}k_BT\frac{\partial \ln\sigma(E)}{\partial E}\bigg|_{E=E_F}. \tag{4}$$

The energy-dependent conductivity is generally represented by

$$\sigma(E)=n(E)|e|\mu(E), \tag{5}$$

where $n(E)$ is the carrier density and $\mu(E)$ is the mobility contributing to $\sigma(E)$. If μ is assumed to be independent of energy, Eq. (4) becomes

$$S(T)=\frac{\pi^2}{3}\frac{k_B}{|e|}k_BT\frac{N(E_F)}{n(E_F)}=\frac{\pi^2}{3}\frac{k_B}{|e|}k_BT\eta(E_F), \tag{6}$$

where $N(E_F)$ is the DOS at the Fermi level as defined in Eq. (2) and $\eta(E_F)$ is the DOS at the Fermi level per carrier. Hence the values of $\eta(E_F)$ for I_2-D, E, I_2-E, and G can be estimated from the slope of the plots of $S(T)$ and are listed in the second column of Table IV. Furthermore, using the values of $N(E_F)$ in Table III, $n(E_F)$ can be evaluated and is also given in Table IV. On the other hand, one can evaluate $n(E_F)$ for I_2-D and I_2-E using the [I]/[C] molar ratio in Table I on the assumption that the dopant species is I_3^- as in polyacetylene[17] and that charge transfer from the carbon skeleton to the dopants is complete. It is seen from Table IV that this assumption works well for I_2-E but not for I_2-D. This discrepancy suggests that in I_2-D only a very small number of absorbed iodine molecules can act as an electron acceptor, possibly because the structure with undeveloped graphitization cannot fully accommodate the dopants.

Extrapolation of the plot of $S(T)$ for G demonstrates a small intercept (-1.8 μV/K), signifying, for instance, that μ is energy dependent. In this case, Eq. (6) has an additional term as follows:

$$S(T)=\frac{\pi^2}{3}\frac{k_B}{|e|}k_BT\left[\eta(E_F)+\frac{\partial \ln\mu(E)}{\partial E}\bigg|_{E=E_F}\right]. \tag{7}$$

One might argue that this term arises from thermally activated process such as hopping similar to the cases of $Ce_{3-x}S_4$ ($x=\frac{1}{3}$)[18] and $La_{1-x}SrVO_3$ ($x=0.20$).[19] Assuming

TABLE III. Exponential factor (T_0 in K) of Eq. (2) and estimated DOS at the Fermi level [$N(E_F)$ in states /eV cm^3] evaluated from $T^{-1/4}$ dependence of σ.

Sample	T_0 Pristine	T_0 I_2-doped	T_0 Na-doped	$N(E_F)$ Pristine	$N(E_F)$ I_2-doped	$N(E_F)$ Na-doped
B	1.1×10^9	3.3×10^8	3.2×10^7	1.7×10^{17}	5.6×10^{17}	5.8×10^{18}
D	1.8×10^8	7.6×10^7	5.2×10^6	1.1×10^{18}	2.4×10^{18}	3.6×10^{19}
E	3.3×10^6	4.7×10^5	3.7×10^4	5.7×10^{19}	4.0×10^{20}	5.0×10^{21}
G[a]	5.2×10^2	8.9×10^1	3.1×10^2	3.6×10^{23}	2.1×10^{24}	5.9×10^{23}

[a]See text with respect to the value of $N(E_F)$ of G series.

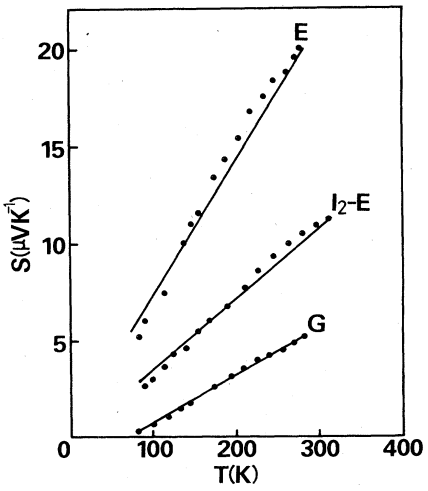

FIG. 6. Temperature dependence of thermoelectric power of E with a fitting curve $S(T)=0.072T$, I_2-E with $S(T)=0.036T$, and G with $S(T)=0.025T-1.8$.

$$\mu(E)=\mu_0 \exp\left[-\frac{W(E)}{k_B T}\right], \tag{8}$$

where μ_0 represents the energy-independent term, $\partial W(E)/\partial E \mid_{E=E_F}$ is estimated to be 6.4×10^{-3} by the substitution of Eq. (8) into Eq. (7). This value is considerably small, and hence $\mu(E)$ in G could be regarded to be almost energy independent.

C. Magnetoresistance

As described in Sec. III A, the 3D-VRH mechanism does not work in G-series samples as a whole. Hence, we have examined transverse magnetoresistance of G and I_2-G at 4.2 K so as to obtain information on the Fermi energy surface of these.

The measured magnetoresistance rate (MR), defined by

$$\frac{\Delta\rho}{\rho_0}\equiv\frac{\rho(B)-\rho_0}{\rho_0}, \tag{9}$$

is plotted in Fig. 7 versus B^2, where $\rho(B)$ and $\rho(0)$ are the resistances under magnetic fields B and zero field, respectively. Both G and I_2-G demonstrate positive MR for all ranges of B. This feature is common to other pyrolized carbon such as heated coke or bamboo char treated at about 900 °C.[20] It is interesting to note that positive MR shown by bamboo char has been ascribed to the 3D-VRH conduction therein.[20] On the other hand, positive MR and the 3D-VRH mechanism are obviously uncorrelated in the present samples. The MR curves of both G and I_2-G linearly change with B^2 and tend to saturate at higher fields, which suggests that the Fermi energy surface is closed in both samples.

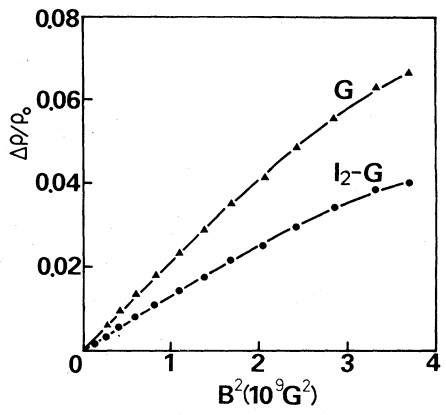

FIG. 7. Magnetic field dependence of $\Delta\rho/\rho_0$ in G and I_2-G at 4.2 K.

Employing the relationship proposed by Soule,[21]

$$\frac{\Delta\rho}{\rho_0}=\mu_{\text{eff}}^2 B^2, \tag{10}$$

μ_{eff} (effective mobility) of G and I_2-G can be estimated. Furthermore, using the relations

$$\sigma=\sigma(E_F)=N(E_F)\mid e\mid \mu_{\text{eff}} k_B T, \tag{11}$$

the DOS at the Fermi level (at 4.2 K) is evaluated with respect to G and I_2-G. The results are listed in Table V, where the magnitudes of $N(E_F)$ are more realistic than those in Table III estimated from the $T^{-1/4}$ analysis of $\sigma(T)$.

It is noted that μ_{eff} of I_2-G is less than that of G, probably due to scattering of carriers by dopant molecules. Hence, it is concluded that the increase in σ of I_2-G arises from the increase in the number of carriers upon doping as indicated by the magnitude of $N(E_F)$ in Table V.

TABLE IV. DOS at the Fermi level per carrier [$\eta(E_F)$ in states/eV carrier] from the data of $S(T)$ and carrier density at the Fermi level [$n(E_F)$ in carriers per carbon atom].

Sample	$\eta(E_F)$	$n(E_F)$ from $N(E_F)$ in Table III[a]	$n(E_F)$ from [I]/[C] in Table I
I_2-D	8.56	9.2×10^{-6}	1.7×10^{-3}
E	2.95	6.5×10^{-4}	
I_2-E	1.47	9.7×10^{-3}	7.3×10^{-3}
G	1.02	3.5×10^{-3}	

[a]For G, $N(E_F)$ estimated from the magnetoresistance data (see Sec. III C) is adopted.

TABLE V. Effective mobility (μ_{eff} in $\text{cm}^2/\text{V sec}$) and DOS at the Fermi level [$N(E_F)$ in states/eV cm^3] evaluated from magnetoresistance data at 4.2 K along with σ (in S cm^{-1}) for G and I_2-G.

Sample	μ_{eff}	$N(E_F)$	σ
G	450	1.2×10^{20}	3.16
I_2-G	360	1.0×10^{21}	2.14×10^{1}

IV. CONCLUDING REMARKS

Transport properties have been examined with respect to pristine and heavily doped polyacenic materials prepared by pyrolytic treatment of PF resin under various temperatures (T_p). There are five major features in the present study.

(1) The sample prepared under lower T_p ($\simeq$600 °C) demonstrates the behavior of $\sigma(T)$ governed by the 3D-VRH mechanism even after the heavy doping thereupon. But the thermoelectric power of this sample is rather temperature independent.

(2) For the samples prepared under higher temperatures (650—800 °C) the 3D-VRH mechanism is less likely to occur, as seen in the $\sigma(T)$ plots. Temperature dependence of thermoelectric power gradually reflects the intrinsic nature of the nearly-filled-band metallic system.

(3) The thermally activated conduction mechanism prevails in the sample with $T_p = 935$ °C. The activation energy is of the order of 10^{-3} eV, being one order less than $k_B T$ at room temperature, which permits a metallic behavior of this material at a higher temperature range. The magnitude of thermoelectric power at room temperature demonstrates an intrinsic semiconductor-metallic transition at this sample.

(4) The magnetoresistance of this sample is positive and tends to saturate at higher magnetic fields. This suggests that the Fermi-energy surface is closed in this sample. The estimated mobility of the sample from magnetoresistance is considerably large.

(5) All the pristine samples are p type on the basis of the sign of thermoelectric powers. This signifies that there are some intrinsic acceptor levels in all of the pristine samples, reflecting their structures.

These findings in the transport properties of the studied polyacenic semiconductive materials offer some illumination for understanding the solid-state properties and structures of these materials. Currently we suppose that the structure of the present material is polycrystalline, consisting of mixed polyacenic skeletons, some of which make metallic fragments. In the low-T_p material these skeletons are not well developed, and hence the 3D-VRH mechanism is dominant. With higher T_p, polyacenic skeletons develop and become larger in size, which demonstrates polycrystalline nature more clearly.

It is rather surprising that the doping process is efficient in such disordered materials, which may open up a new individual area of organic amorphous semiconductors. Further detailed analyses such as direct measurements of mobility of the present samples using Hall-effect (for samples with higher T_p) and time-of-flight methods (for samples with lower T_p) are in progress. These results, as well as individual reports of the measurements of thermoelectric power and magnetoresistance, will be published in the near future.

ACKNOWLEDGMENT

This work was partially supported by Grant-in-Aid for Scientific Research from the Ministry of Education, Science, and Culture of Japan.

[1]H. Shirakawa, E. J. Louis, A. G. MacDiarmid, C. K. Chiang, and A. J. Heeger, J. Chem. Soc. Chem. Commun. 578 (1977); C. K. Chiang, C. R. Fincher, Jr., Y. W. Park, A. J. Heeger, H. Shirakawa, E. J. Louis, S. C. Gau, and A. G. MacDiarmid, Phys. Rev. Lett. **39**, 1098 (1977); C. K. Chiang, M. A. Druy, S. C. Gau, A. J. Heeger, E. J. Louis, A. G. MacDiarmid, Y. W. Park, and H. Shirakawa, J. Am. Chem. Soc. **100**, 1013 (1978).

[2]See, for example, J. C. W. Chien, *Polyacetylene—Physics, Chemistry and Material Science* (Academic, New York, 1984), and references therein.

[3]J. M. Pochan, D. F. Pochan, H. Rommelmann, and H. W. Gibson, Macromolecules **14**, 110 (1981).

[4]L. W. Shacklette, R. R. Chance, D. M. Ivory, G. G. Miller, and R. H. Baughman, Synth. Met. **1**, 307 (1979/80).

[5]K. Kaneto, K. Yoshino, and Y. Inuishi, Jpn. J. Appl. Phys. **21**, L567 (1982); J. Chem. Soc. Chem. Commun. 382 (1983); G. Tourillon and F. Garnier, J. Electroanal. Chem. **135**, 173 (1982).

[6]T. Yamabe, K. Tanaka, K. Ohzeki, and S. Yata, J. Phys. (Paris) Colloq. Suppl. No. 6, **44**, C3-645 (1983); K. Tanaka, K. Ohzeki, T. Yamabe, and S. Yata, Synth. Met. **9**, 41 (1984).

[7]K. Tanaka, K. Yoshizawa, T. Koike, T. Yamabe, J. Yamauchi, Y. Deguchi, and S. Yata, Solid State Commun. **52**, 343 (1984); K. Tanaka, T. Koike, T. Yamabe, J. Yamauchi, Y. Deguchi, and S. Yata, Polym. Prep. (Jpn.) **33**, 2479 (1984) (in Japanese).

[8]W. Bücker, J. Non-Cryst. Solids **12**, 115 (1973).

[9]See S. Yata (Kanebo Ltd.), European Laid-Open Patent Publication, No. 0067444.

[10]N. F. Mott and E. A. Davis, *Electronic Processes in Non-Crystalline Materials,* 2nd ed. (Clarendon, Oxford, 1979), Chap. 2.

[11]K. Tanaka, M. Ueda, T. Yamabe, and S. Yata, Polym. Prep. (Jpn.) **33**, 2475 (1984) (in Japanese).

[12]N. F. Mott, Rev. Mod. Phys. **50**, 203 (1978).

[13]J. J. Hauser, J. Non-Cryst. Solids **23**, 21 (1977).

[14]M. Murakami, H. Yasujima, Y. Yumoto, S. Mizogami, and S. Yoshimura, Solid State Commun. **45**, 1085 (1983).

[15]Y. W. Park, A. Denenstein, C. K. Chiang, A. J. Heeger, and A. G. MacDiarmid, Solid State Commun. **29**, 747 (1979); Y. W. Park, A. J. Heeger, M. A. Druy, and A. G. MacDiarmid, J. Chem. Phys. **73**, 946 (1980).

[16]J. M. Ziman, *Principles of the Theory of Solids,* 2nd ed. (Cambridge University Press, Cambridge, 1972), Chap. 7.

[17]T. Matsuyama, H. Sakai, H. Yamaoka, Y. Maeda, and H. Shirakawa, Solid State Commun. **40**, 563 (1981).

[18]M. Cutler and N. F. Mott, Phys. Rev. **181**, 1336 (1969).

[19]P. Dougier and A. Casalot, J. Solid State Chem. **2**, 396 (1970). See, also, Chap. 4 of Ref. 10.

[20]Y. Hishiyama, Y. Kaburagi, and A. Ono, Carbon **17**, 265 (1979).

[21]D. E. Soule, Phys. Rev. **112**, 698 (1958).